

# MODELING THE THERMAL AND CHEMICAL EVOLUTION OF THE MARTIAN LITHOSPHERE OVER TIME

F. Clare McGroarty, Megan S. Duncan (advisor)

Department of Geosciences, Virginia Tech

926 West Campus Dr. 4044 Derring Hall Blacksburg, VA 24061

## Abstract

Mars is a particularly ideal planet to study planetary evolution and development; as its crust has been preserved over its history, rather than recycled through subduction as happens on Earth. In order to attain a more coherent understanding of martian evolution, we focused on the history of the martian lithosphere. We developed a model that calculates the thermal history and melt composition of Mars over time. This model provides insight into the planet's history and enables us to see how the density and seismic properties have evolved over time. We calculated the temperature profile through the lithosphere and then fit an equation to pre-existing data in order to produce a model to predict the composition of a melt produced at a calculated pressure and temperature. From the model, we see a trend of decreasing mafic composition over time. We calculated the density and seismic properties of the lithosphere and found that they decrease over time; this result matches the observations recently made by NASA's InSight mission.

## Introduction

Planetary evolution is one of the many mysteries of the developing universe, and it can be one of the most difficult processes to study. Exoplanets are too far away to study effectively, and the other planets of the solar system are not yet well constrained. The Earth is not an ideal location to study planetary evolution, as its crust regularly recycles itself through subduction processes. Mars is thus an ideal location to study planetary evolution, as there is no history of plate tectonics or crustal recycling and the planet's entire historical crust is present. Understanding the evolution of Mars

will help us to understand how planets and solar systems evolve, including how the Earth may have evolved over time.

However, there are currently few observed constraints on martian thermal and geochemical evolution. Studying martian evolution will help us to understand how the other planets, including the Earth, may have evolved over time, as well as why the other planets have evolved differently than the Earth (such as not developing plate tectonics). Knowledge of the planet is limited to data from orbital scans (spectroscopy), surface measurements (rovers and landers), and meteorite studies. These sources are limited to the surface conditions of Mars, but provided key information about the crust.

## Previous Constraints

### Crustal properties

The surface composition of Mars is generally basaltic, with measured abundances of heat producing elements (HPEs) of 0.18 ppm uranium, 0.7 ppm thorium, and 3740 ppm potassium [1]. The average crustal thickness is ~50 km, with variation from ~3 to >100 km [e.g., 2, 3]. In the Noachian, the average crustal thickness was ~20 km [4].

Age estimates of the surface were determined via crater-counting, with the oldest surfaces in the Southern Highland of over 3 billion years old, while the most recent lava flows are significantly younger at <1 Ma, indicating the potential for localized activity today [5, 6].

### Thermal properties

Using measured surface and meteorite compositions, previous work determined the mantle potential temperature ( $T_p$ ) decreased from ~1450 °C to ~1375 °C over the past 4.5

Gy [7], indicating that the planet cooled overall through time.

The surface heat flux also decreased over time, from about 50 mW/m<sup>2</sup> 4.5 Ga to 26 mW/m<sup>2</sup> in the present day [8]. However, other constraints on the heat flux over time indicate that the modern heat flux is about 20 mW/m<sup>2</sup>, and about 50 mW/m<sup>2</sup> 4 Ga [9-11]. There is variation in the surface heat flow in the present day from 14 mW/m<sup>2</sup> to 25 mW/m<sup>2</sup>, indicating a range of heat flow across the planet [9, 12]. In [12], the largest uncertainty in the heat flux was due to uncertainty in the size of the martian core; previous constraints on the martian interior left uncertainty on the size, phase (solid or liquid), and composition (amount of sulfur) in the core. NASA's InSight mission, through seismic studies, has recently determined that the martian core is liquid and that the parameters from [13] predicting about the radius to be ~1840 km, from which we will be able to place constraints on the sulfur content. These results will change the surface heat flows above, but this is outside the scope of this study and we will use the current values to constrain our models; InSight to date has been unable to measure the heat flow through the crust. We used the global average heat flow in our models, allowing room for local variation; [9] acknowledges that the average heat flux can vary from location to location based on the presence or absence of mantle plumes under a particular location.

#### Results from InSight

As stated above, crustal thickness estimates vary from 3 to 100 km, with an average of 50 km. The current InSight mission refined this global average range based on seismic observations to 24–40 km if the crust is dominated by two seismically distinct layers, and 35–72 km if three layers [14]. They further detected the layer boundaries at 10 km and 22 km marked by sharp increases in seismic velocities [15]. They also determined the lithosphere thickness to be ~500 km at the InSight location that is characterized by a

negative slope in  $V_S$  and neutral to slightly positive slope in  $V_P$  [16].

The team also calculated ranges for crustal enrichment (HPEs) and found that in order to match the melt volume today (i.e., melting only at Tharsis) that crustal enrichments ( $\Delta$ ) should vary from 20–22 for the two layer model and 11–14 for the three layer model. This leads to Th concentrations of 1200–1700 ppb or 680–1050 ppb for the two and three layer model, respectively, with the caveat that the two layer model would require an enriched HPE layer in the lower crust [17]. Therefore, the three layer model is preferred. Maximum crustal densities were determined to be 2900 kg/m<sup>3</sup> for the two layer model and 3100 kg/m<sup>3</sup> for the three layer model, with a minimum of 2550 kg/m<sup>3</sup>, which are similar estimates based off of previous Moment of Inertia constraints [18]. They note that these values are less than the calculated densities of the shergottites, and several previous estimates for the bulk crust [e.g., 19], but are not unreasonable considering impart gardening porosity, the presence of widespread clays, and water ice that are likely present for the first few km of Mars' crust [e.g., 20].

Here we produced a model that would resolve some of these questions and inform us how the martian crust has evolved over time. The end result of this model is a self-consistent process that relies on both geochemical and geodynamic methods to model heat flow through the martian lithosphere over time, the global average melt produced over time, the composition of the melts, and the mineral composition and corresponding density and seismic properties.

#### Methods

We used both geochemical and geophysical methods to produce our model. We chose to utilize both disciplines in order to produce a self-consistent model that would yield more realistic results. All calculations represent global averages, none of the

geochemical or geodynamic thermal profiles are intended to represent any specific location on Mars. Using previously determined constraints, we built a simplified geochemical model whose results were compared to our 3D convection model moving toward a self-consistent geochemical-thermal-convection model for Mars. The geochemical model consisted of several parts: 1) areotherm calculations, 2) construction of a melt model based on previous experiments, and 3) Perple\_X modeling to determine  $\rho$ ,  $V_P$ , and  $V_S$  profiles through the crust and mantle lithosphere.

### Areotherms

The first stage involved calculating areotherms, or temperature profiles through the conductive crust and mantle lithosphere. The areotherm calculations were built off of well-established parameters, originally designed for the Earth, with the appropriate modifications for Mars. Our reference model was built for present day Mars and consisted of a single, 50 km thick crust of the average crust composition [1], and an undepleted mantle lithosphere composition of Dreibus and Wänke [21], i.e., homogenous HPE concentrations. Using these concentrations, we can determine the amount of heat produced in the crust and mantle lithosphere. We calculated the areotherms using the methods in [22], according to the equation:

$$T(z) = T_0 + \frac{q_i \Delta z_i}{k_i} - \frac{A_i \Delta z_i^2}{2k_i} \quad (1)$$

where  $T_0$  is the surface temperature ( $\sim 220$  K),  $k$  is thermal conductivity ( $\sim 3.2$  W/mK),  $q$  is the surface heat flow ( $\sim 25$  mW/m<sup>2</sup> in the present day),  $z$  is the depth in km, and  $A$  is the heat production from HPEs (U, Th, K, in fraction). The areotherms were combined with the adiabat calculations from [7]; the intersection of the areotherm and adiabat marked the base of the thermal lithosphere. These calculations for the areotherm and adiabat were performed

at one billion year intervals from 4 Ga to the present day (0 Ga).

The areotherms and adiabats were used to calculate the melt percent ( $F$ ) at each timestep using the equation:

$$\frac{F}{P_0 - P_F} = \frac{\frac{dT}{dP_{\text{solidus}}} - \frac{dT}{dP_{\text{adiabat}}}}{\frac{\Delta H_F}{C_P} + \frac{dT}{dF}} \quad (2)$$

where  $P_0$  is the pressure in GPa where the solidus [23] intersects the adiabat, which indicates the initiation of melt production,  $P_F$  is the pressure at the cessation of melt production and is marked by the intersection of the adiabat and the areotherm, or the base of the lithosphere,  $dT/dP_{\text{solidus}}$  is the slope of the solidus (106.15 K/GPa over the pressure range here [23]),  $dT/dP_{\text{adiabat}}$  is the slope of the adiabat (0.18 K/km [7]),  $\Delta H_F$  is the enthalpy of fusion ( $6.4 \times 10^5$  J/kg [24]),  $C_P$  is the heat capacity (1200 J/K kg [24]), and  $dT/dF$  is the change in temperature as a function of melt fraction and was calculated from previous experimental data [25, 26], ranging from 4.38 to 3.9 K/F, depending on pressure.

### Melt model

We used the previous experimental results for mantle melting in

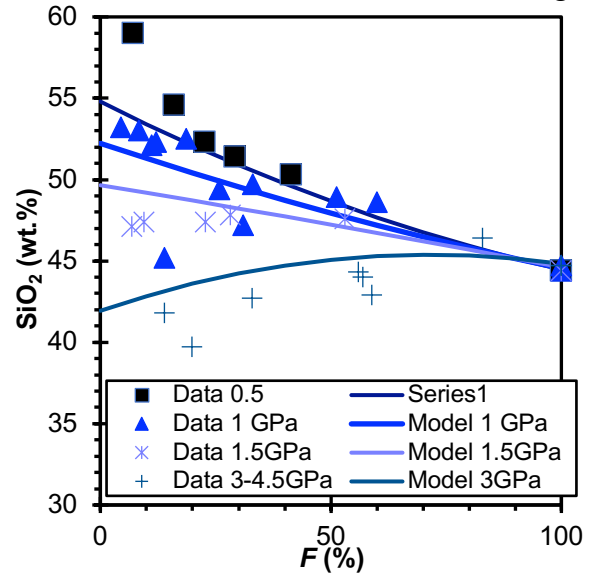


**Figure 1.** Previous experimental data (symbols) with our calculated regressions (lines) for SiO<sub>2</sub>. The data and model is divided into pressure bins in order to show how the model fits at each experimental pressure range.

Mars [25, 26], which reported melt composition over a range  $T$ ,  $P$ , and  $F$ , to fit a model of melt composition as a function of  $P$  and  $F$  (Fig. 1). We began by using the equation form for peridotite melting from Duncan, Dasgupta [27] for each oxide. Equation form was modified on an oxide basis, if the experimental data indicated importance of the  $P$  terms. We used least squares regression to solve for the coefficients of the model equations. Using the above calculation of  $P_F$  and  $F$  over time, we calculated the composition of the melt at each time interval and used mass balance principles to calculate the composition of the residual un-melted material. We made the simplifying assumption that all melt produced was solidified into crust, while the residual, un-melted material formed the mantle lithosphere. Based on these outputs, we adjusted the areotherms as needed (removing  $K$  from the mantle lithosphere as indicated by the melt model).

### Mineralogical calculations

We used our calculated melt and residual compositions, and our reference surface and mantle lithosphere compositions [1, 21] to calculate the mineral composition, density, and seismic velocities of the crust and mantle lithosphere at each time step using `Perple_X`. We used the `hpha622` dataset and corresponding solution models to calculate the mineral modes and lithospheric properties over the  $P$ - $T$  range of our areotherms. We compared our reference case to the results from [28] to ensure similar results. In order to produce a reference case, we followed the methods of [28] to produce the density and mineral plots. In order to accurately calculate the density and seismic velocities in the crust, we had to modify the methods. Due to the low temperatures of the crust, we calculated the mineral modes of the crust at a higher temperature; because the melt crystallized at a higher temperature than what is currently in the crust, and because the mineral modes have not

changed since crystallization, we can use these mineral modes calculated at higher temperature to calculate the density. We used the same

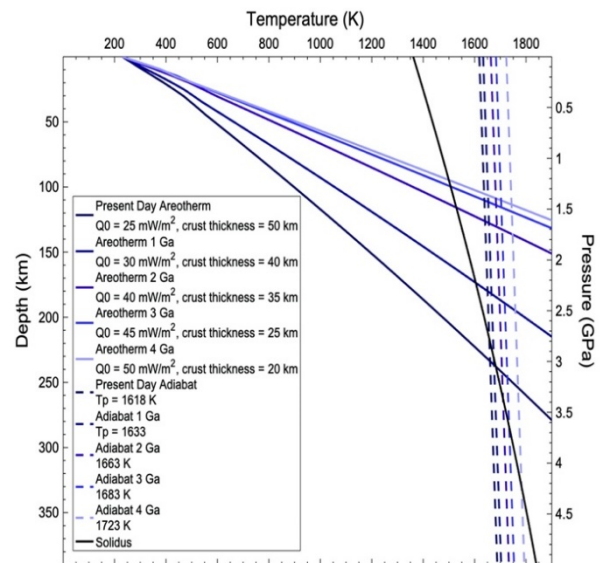


**Figure 2.** Calculated areotherms (solid lines) and adiabats (dashed lines) through time. Darker colors represent the present day and the lines lighten through time so that the lightest color represents the areotherm/adiabat at 4 Ga. The solidus is the solid black line. The solidus/adiabat/areotherm intersections in the modern day indicate that little to no melt is being produced in the present day.

constants and equations as in [29] in order to calculate the density at the areotherm temperature and pressure, using the mineral modes calculated that the higher temperature. This method allowed us to calculate the density and seismic velocity of the crust based on the more accurately produced mineral modes.

### Results

The calculated areotherms show a trend of cooling and thickening of the crust and mantle lithosphere over time in the geochemical models (Fig. 2). In the geochemical models, the depth of the lithosphere increases from about 100 km 4 Ga to about 240 km in the present day. At 4 Ga, the adiabat crosses the solidus at ~300 km, decreasing through time, until the present day

where they do not cross indicating melting is not occurring, on average today. This leads to a corresponding decrease in  $F$  over time. In the areotherm from 4 Ga, the adiabat crosses the solidus over a wide range before cross the areotherm. This corresponds to a melt production of 35% across the planet. In the present day, however, there is no point along the temperature profile that crosses the solidus, which corresponds to a totally solid planet with no melt production.

Based on the calculated  $F$  values, we calculated the oxide composition in the melts over time (Fig. 3). The melt compositions become less ultramafic and more mafic with time, decreasing in  $\text{SiO}_2$ ,  $\text{FeO}$ , and  $\text{MgO}$ , coupled with an increase in  $\text{Na}_2\text{O}$ ,  $\text{K}_2\text{O}$ ,  $\text{CaO}$ , and  $\text{Al}_2\text{O}_3$ . These changes also correspond to a change in the seismic velocity and density over time; the seismic velocities decrease over depth, as well as the density.

### Discussion

From the areotherms, we see that the melt fraction decreased over the past four billion years. As the  $F$  decreased, there has also been a change in the melt composition over time. The melt becomes less silicic over time, while simultaneously becoming enriched in

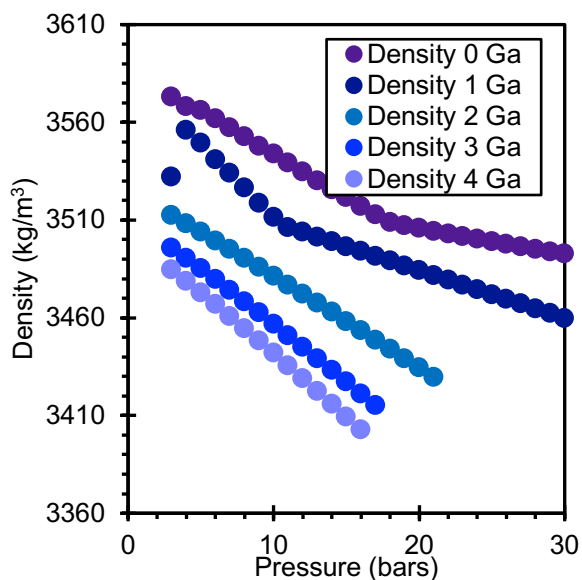


**Figure 3.** Calculated density of the mantle lithosphere as a function of pressure.

$\text{Al}_2\text{O}_3$ ,  $\text{CaO}$ , and  $\text{Na}_2\text{O}$ . The decrease in melt quantity is also correlated to changes in the density and seismic velocity over time; the planet's lithosphere becomes overall denser with time and the  $V_P$  and  $V_S$  also increase over time. More importantly, the  $V_P$  and  $V_S$  modeled follow the same trends as observed by NASA's InSight mission [16] as both  $V_P$  and  $V_S$  decrease with depth (Fig. 5).

The planet's melt cooled and crystallized over the past four billion years. Based on the intersection of the solidus and mantle adiabat from Filiberto [7], we found that there was significantly more melt generated in the past than in more recent

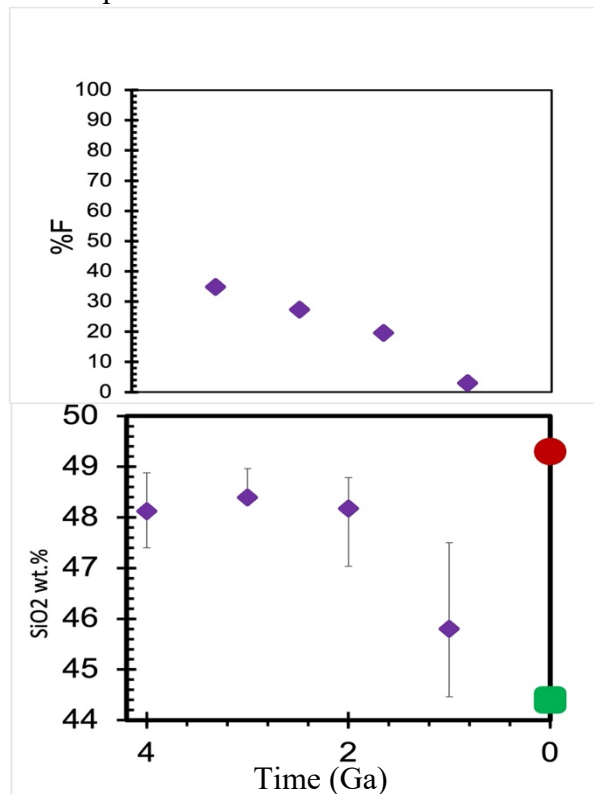


**Figure 3.** Plot demonstrating change in  $F\%$  and  $\text{SiO}_2$  wt. % over time. The green marker represents the  $\text{SiO}_2$  in the undepleted mantle, while the red marker represents the measured  $\text{SiO}_2$  composition on the planet's surface.

times, with no melt on average being produced today. This means that in the present day, there is no magma ocean on Mars, although there is still the possibility for small

amounts of melt to be produced due to local fluctuations in temperature/pressure conditions (or due to presence of a mantle plume).

### Relevance to InSight

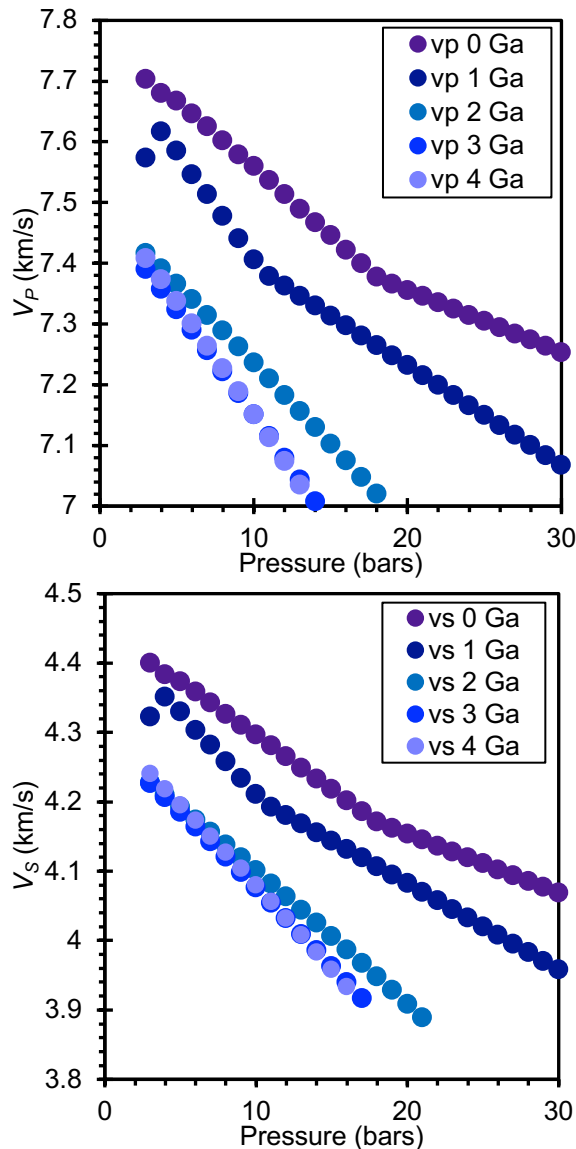


**Figure 4.** Comparison of calculated  $V_P$  (top) and  $V_S$  (bottom) over time. The darkest colors represent the present day and the lightest colors represent 4 Ga. The plots indicated that  $V_P$  and  $V_S$  decrease over depth as well as decrease going back through time.

This research is pertinent to InSight by calculating the seismic profiles through the crust and mantle lithosphere. The heat flow

calculations used in the areotherm inputs are from the Elysium Planitia, which is where the InSight lander is located. Although the results are for a global average lithospheric thickness, the heat flow inputs used are from the location of the InSight lander. Since landing, InSight has found that the martian core is entirely liquid, indicating that the sulfur content is high, likely about 18 wt.% [30]. Our results relate back to InSight by showing mathematically what we can expect/did expect the lander to observe. The models that we have produced provide a comparison between InSight's observed conditions and the predicted model equations. By using the comparison to the InSight observations as an accuracy check, we can confirm the accuracy of the model over time, making the models a more reliable starting point for understanding how the martian mantle and lithosphere have evolved over time. From that comparison to InSight, we can also determine the accuracy of our model predictions of how the martian lithosphere has evolved; because our model is very similar to what is observed by InSight today, we can use it more reliably to look at Mars over its history.

### Conclusions

From these models, we have a clearer vision of how the martian lithosphere evolved over time. While more data and experiments are necessary to refine and enhance this model, we can see from the available data and experiments how the lithosphere has changed compositionally over time. The melt production has decreased in quantity and has similarly seen decreases in Mg and Fe over time; likely due to Fe- and Mg-rich minerals such as olivine and pyroxene melting and crystallizing out of the upper mantle and into the crust over time. These models help us understand how Mars has evolved over time from an initially homogenous mantle composition to the conditions observed on the surface today.

### Acknowledgements

We would like to thank the Virginia Space Grant Consortium for supporting this research. We also thank Mark Caddick and Jonathan Prouty for their assistance with `Perple_X`, and Priyanka Bose for her assistance with the areotherm code.

### References

1. Taylor, S.R. and S. McLennan, *Mars: Crustal composition and evolution, in Planetary Crusts: Their Composition, Origin and Evolution*. 2009, Cambridge University Press. p. 141-180.
2. Wiczorek, M.A. and M.T. Zuber, *Thickness of the martian crust: Improved constraints from geoid-to-topography ratios*. *Journal of Geophysical Research-Planets*, 2004. **109**(E01009).
3. Neumann, G.A., et al., *Crustal structure of Mars from gravity and topography*. *Journal of Geophysical Research-Planets*, 2004. **109**(E08002).
4. Norman, M.D., *The composition and thickness of the crust of Mars estimated from rare earth elements and neodymium-isotopic compositions of Martian meteorites*. *Meteoritics & Planetary Science*, 1999. **34**(3): p. 439-449.
5. Werner, S.C., *The global martian volcanic evolutionary history*. *Icarus*, 2009. **201**(1): p. 44-68.
6. Hartmann, W.K., *Martian cratering 8: Isochron refinement and the chronology of Mars*. *Icarus*, 2005. **174**(2): p. 294-320.
7. Filiberto, J., *Geochemistry of martian basalts with constraints on magma genesis*. *Chemical Geology*, 2017. **466**: p. 1-14.
8. Baratoux, D., et al., *Thermal history of Mars inferred from orbital geochemistry of volcanic provinces*. *Nature*, 2011. **472**(7343): p. 338-41.
9. Parro, L.M., et al., *Present day heat flow model of Mars*. *Scientific Reports*, 2017. **7**: p. 45629.
10. McGovern, P.J., et al., *Localized gravity/topography admittance and correlation spectra on Mars: Implications for regional and global evolution*. *Journal of Geophysical Research-Planets*, 2002. **107**(E12, 5136).
11. McGovern, P.J., et al., *Correction to "Localized gravity/topography admittance and correlation spectra on Mars: Implications for regional and global evolution"*. *Journal of Geophysical Research-Planets*, 2004. **109**(E07007).
12. Plesa, A.C., et al., *How large are present-day heat flux variations across the surface of Mars?* *Journal of Geophysical Research-Planets*, 2016. **121**(12): p. 2386-2403.
13. Khan, A., et al., *A geophysical perspective on the bulk composition of Mars*. *Journal of Geophysical Research: Planets*, 2018. **123**(2): p. 575-611.
14. Wiczorek M. A., K.-E.B., Panning M. P., Plesa A.-C., McLennan S. M. *Global Character of the Martian Crust as Revealed by InSight Seismic Data*. in *Lunar and Planetary Science Conference*. 2021.
15. Lognonné, P., et al., *Constraints on the shallow elastic and anelastic structure of Mars from InSight seismic data*. *Nature Geoscience*, 2020. **13**(3): p. 213-220.
16. Khan A., C.S., van Driel M., Giardini D., Lognonne P. *Constraints on the Martian Upper Mantle from InSight Seismic Data*. in *Lunar and Planetary Science Conference*. 2021. Online.
17. Michaut C., P.A.-C., Samuel H., Wiczorek M. A., McLennan S. *Crustal Radioactivity on Mars Constrained by InSight Data and Geodynamic Modeling*. in *Lunar and Planetary Science Conference*. 2021.
18. Sohl, F., G. Schubert, and T. Spohn, *Geophysical constraints on the composition and structure of the martian*

- interior*. Journal of Geophysical Research-Planets, 2005. **110**(E12008).
19. Goossens, S., et al., *Evidence for a low bulk crustal density for Mars from gravity and topography*. Geophysical Research Letters, 2017. **44**(15): p. 7686-7694.
  20. Baratoux, D., et al., *Petrological constraints on the density of the martian crust*. Journal of Geophysical Research-Planets, 2014. **119**(7): p. 1707-1727.
  21. Dreibus, G. and H. Wänke, *Mars, a volatile rich planet*. Meteoritics, 1985. **20**(2): p. 367-381.
  22. Rudnick, R.L., W.F. McDonough, and R.J. O'Connell, *Thermal structure, thickness and composition of continental lithosphere*. Chemical Geology, 1998. **145**(3-4): p. 395-411.
  23. Duncan, M.S., et al., *Extending the solidus for a model iron-rich martian mantle composition to 25 GPa*. Geophysical Research Letters, 2018. **45**(19): p. 10211-10220.
  24. Kiefer, W.S., *Melting in the martian mantle: Shergottite formation and implications for present-day mantle convection on Mars*. Meteoritics & Planetary Science, 2003. **38**(12): p. 1815-1832.
  25. Collinet, M., et al., *Melting of the primitive martian mantle at 0.5-2.2 GPa and the origin of basalts and alkaline rocks on Mars*. Earth and Planetary Science Letters, 2015. **427**: p. 83-94.
  26. Matsukage, K.N., et al., *Melting of the martian mantle from 1.0 to 4.5 GPa*. Journal of Mineralogical and Petrological Sciences, 2013. **108**(4): p. 201-214.
  27. Duncan, M.S., R. Dasgupta, and K. Tsuno, *Experimental determination of CO<sub>2</sub> content at graphite saturation along a natural basalt-peridotite melt join: Implications for the fate of carbon in terrestrial magma oceans*. Earth and Planetary Science Letters, 2017. **466**: p. 115-128.
  28. Semprich, J. and J. Filiberto, *High-pressure metamorphic mineralogy of the Martian crust with implications for density and seismic profiles*. Meteoritics & Planetary Science, 2020. **55**(7): p. 1600-1614.
  29. Holland, T. and R. Powell, *An improved and extended internally consistent thermodynamic dataset for phases of petrological interest, involving a new equation of state for solids*. Journal of Metamorphic Geology, 2011. **29**(3): p. 333-383.
  30. Stähler S. C., C.S., Duran A. C., Garcia R. G., Giardini D. . *Seismic Detection of the Martian Core by InSight*. in *Lunar and Planetary Science Conference*. 2021.